REVISTA INTERDISCIPLINAR DE PESQUISA EM ENGENHARIA

CILAMCE 2016

XXXVII IBERIAN LATIN AMERICAN CONGRESS ON COMPUTATIONAL METHODS IN ENGINEERING
BRASÍLIA - DF - BRAZIL

MODAL ANALYSIS OF HYBRID ADAPTATIVE BEAMS

Guilherme Vaz Ferreira

Flaminio Levy Neto

guilhermedf@gmail.com

flaminio@unb.br

University of Brasília

Department of Mechanical Engineering, UnB-FT-ENM, 70910-900, Brasília, DF, Brazil

Abstract. Smart or adaptative structures are those capable to perform some special functions when stimulated externally. In the context of this type of structure, hybrid adaptative composite beams, reinforced with active Ni-Ti filaments, were simulated in the present work. Such beams may be adopted for vibration control, exploring the possibility of changing their bending stiffness by means of controlling the temperature of the shape memory alloy filaments. The main objective of this paper is to present, for a free-free boundary condition, the vibration modes and their frequencies obtained analytically and numerically for prismatic beams, which incorporate nineteen layers of epoxy reinforced with chopped E-glass mat (17 plies), and two symmetric active plies (A) embedded with up to four Ni-Ti wires each (2+A+13+A+2). One particular aspect of this investigation is to verify how the natural frequency of the beams changes, when an electric current passes through the Ni-Ti wires and elevates their temperature from 25 ºC to 69 ºC, converting 100% of the Ni-Ti wires into the more rigid austenitic phase. In order to verify the accuracy of the analytical method, it was compared with two numerical models based on the finite element method. The maximum differences between the methodologies, in module, was 4.50%.

Keywords: SMAHC beam, Modal analysis, Finite element method

1 INTRODUCTION

Conventional polymeric matrix composite materials combine at least two distinct phases, reinforcement as well as an agglutination matrix, and are well known by their high specific strength and stiffness, which allow the creation of extremely light and efficient structural components (Daniel & Ishai, 2006; Levy-Neto & Pardini, 2006). However, if a third active phase is incorporated, smart or adaptative structures, which exhibit special functions when stimulated by external impulses, can be created. The composites investigated in the present study, designated by Rogers & Robertshaw (1989) as Shape Memory Alloy Hybrid Composites (SMAHC), are prismatic beams that incorporate as a third constituent, Ni-Ti active wires. The development of Ni-Ti shape memory alloys (SMA) has paved the way for special applications in robotics, bioengineering and complex aerospace systems (Ghandi & Thompson, 1992; Janocha, 1999; Srinivasan & McFarland, 2001). With the addition of the Ni-Ti wires that, besides other features, increase their elasticity modulus when heated, SMAHC can be regarded as adaptative structures. The development of smart/intelligent composite structures, incorporating SMA, has become an attractive research topic in engineering, due to their capacity to work as a sensor or actuator (Turner, 2000).

Adaptative composite structures with embedded active Ni-Ti wires, are able to respond to external inputs, for example a moderate increase in temperature (e.g. from 25 °C to 69 °C). These SMA wires change their elasticity modulus, by a factor of almost three times, as showed in Fig. 1, when a controlled electric current warms up the wires (Srinivasan & McFarland, 2001). Thus, a SMAHC component can present different mechanical behavior and adapt itself to service and environmental conditions. The controlled variation of the elasticity modulus, presented by SMA, for instance the Ni-Ti alloys, have motivated the application of such special alloys in many situations, for structural as well as machine vibration control and the optimization of different mechanical systems (Otsuka & Wayman, 1998).

The special properties presented by the Ni-Ti alloys depends on the transformation of the crystal structure, from the relatively softer martensitic phase, at lower temperatures (e.g. $T < 25$ °C), to the stiffer austenite phase at higher temperatures (e.g. $T > 69$ °C). During the initial development of Ni-Ti alloys, it was found that a composition consisting of nearly equal numbers of nickel and titanium atoms showed the transformation that leads to shape memory and an increase on the elasticity modulus (E). Further, by adding a slight extra amount of nickel in the alloy, it was possible to change the transformation temperature from near 100 °C down to below 0 °C. In addition, this alloy had constituents that were not prohibitively expensive, and could be produced with existing metalworking techniques. The important temperatures at which phase transformations take place are known as: M_s; M_f; As; as well as A_f, and represent the temperatures of start (s) and finish (f) of martensitic (M) and austenitic (A) transformations, respectively (Srinivasan & McFarland, 2001). The main effect that is explored at the present work is the significant variation in stiffness (E) of the Ni-Ti wires, from E_M , at $T < Ms$ in the martensitic phase, up to $E_A = 3.E_M$ (i.e. up to three times larger), at $T > Af$ in the austenitic phase (Turner, 2000), as presented in Fig. 1. Thus, since the natural frequency of a component depends on its mass and stiffness, this frequency, in a SMAHC with embedded Ni-Ti wires, can be changed controlling the temperature of the wires. Meanwhile, the fabrication of SMAHC is complex and involves three different constituents in the same component. The main objectives of this work are: (i) the development of a fabrication method to produce 7 SMAHC beams; and (ii) evaluate, the elastic properties and

CILAMCE 2016

Proceedings of the XXXVII Iberian Latin-American Congress on Computational Methods in Engineering
Suzana Moreira Ávila (Editor), ABMEC, Brasília, DF, Brazil, November 6-9, 2016

natural frequencies, of SMAHC beams with up to 8 embedded Ni-Ti wires, subjected to static and dynamical loads, at 25 °C (i.e. T < M_f) and to 69 °C (i.e. T > A_f).
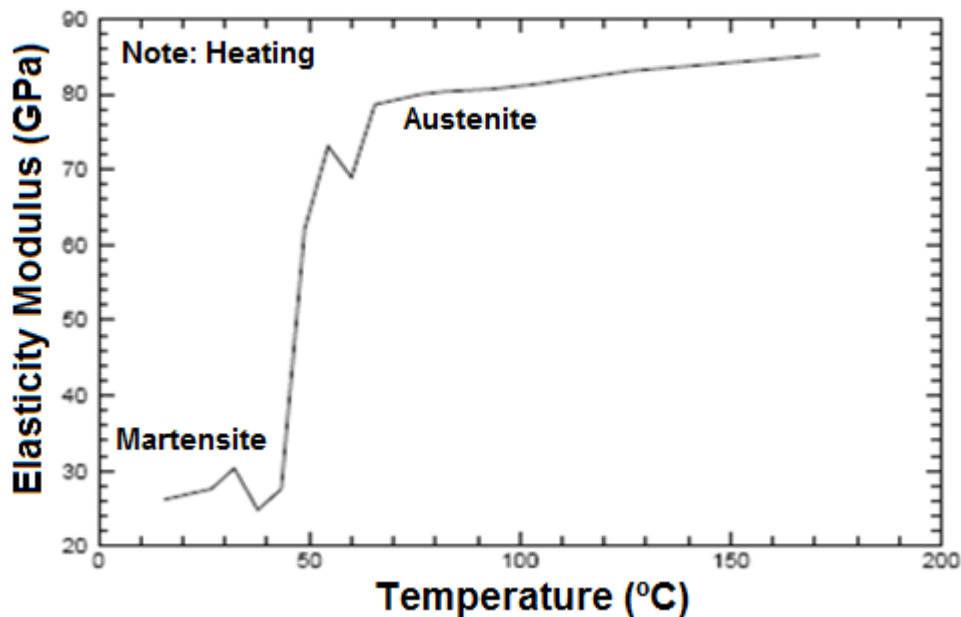

Figure 1. Elasticity Modulus of a Ni-Ti wire from T < Mf up to T > Af (Turner, 2000)

Ni-Ti wires used have the chemical of composition of 55.49 wt% Ni and 44.51 wt% Ti. The starting temperature of the austenite phase is 62 °C (data from Memory-Metalle GmbH manufacturer). The modulus of elasticity in the austenitic phase is 48.4 GPa and in the martensitic phase is 22.7 GPa (Faluhelyi, 2013). The density of the material is 6.45 g/cm^3 (data from Memory-Metalle GmbH manufacturer).

2   MATERIALS AND METHODS

2.1   Fabrication of the beams

Initially, due to its simplicity and low cost, hand layup process without vacuum bag, with consolidation inside closed molds (i.e. male and female combined), was chosen for the fabrication of the SMAHC beams investigated in this work. The constituents adopted were: (i) cold cure (25 °C) and hot cure (80 °C) epoxy resins from Maxepoxi; (ii) E-glass chopped fibers mat; and (iii) Ni(55.49%)–Ti(44.51%) wires from Memory-Metalle GmbH, washed with the reagent Kroll (Faluhelyi, 2013). The basic geometry of the specimens, with length over thickness greater than 16, was based on the ASTM standard D 790-10. An external steel device to keep the Ni-Ti wires stretched during the consolidation of the epoxy matrix was attached to an internal aluminum female mold, as illustrated in Fig. 2.
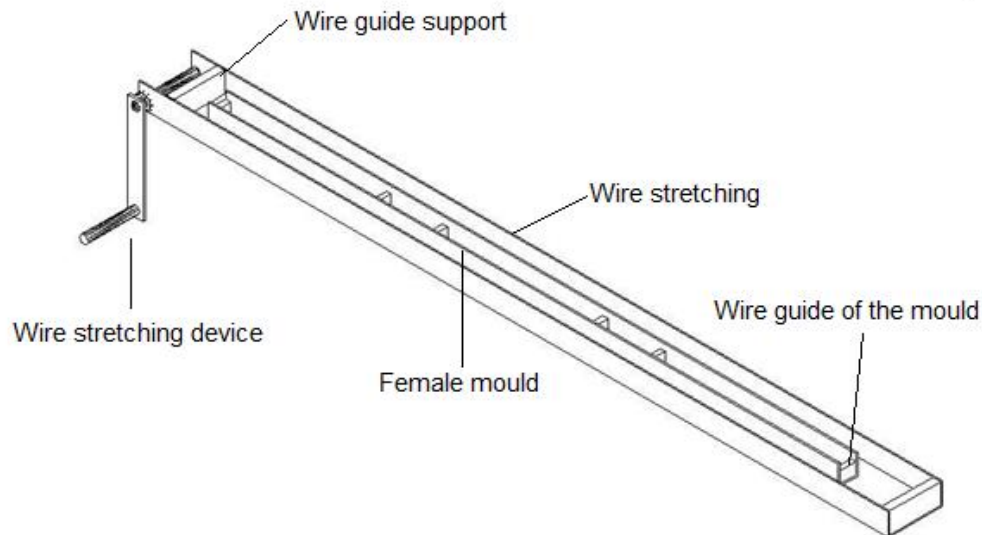
Figure 2. Stretching device and female mold

The female mold presented in Fig. 2 is 1200 mm long and endowed with sets of aluminum blocks with uniformly distributed holes to guide the Ni-Ti wires. It is an U shape aluminum bar, with internal width of 31.3 mm, which is fixed on the steel base wire stretching support. In the fabrication of the beams, one extremity of the wires is fixed in a guiding block and the other end is griped and pulled by the lever of the stretching device. Thus, during the lamination of the E-glass/epoxy plies, the wires are kept straight until the resin is totally cured. As far as the cure temperature of the matrix is concerned, the specimens were divided into two main groups: cold (25 ºC) and hot (80 ºC) cure. For the cold cure group the epoxy system LY1316/HY1208 (glass transition temperature Tg = 60 ºC) was used to impregnate the E-glass mat and Araldite-F/HY956 (Tg = 80 ºC) to impregnate the wires; whereas for the hot cure group the system LY1316/HY1316 (Tg > 80 ºC) was adopted for all the layers. The cure cycle for the cold system is single stage, 24 hours at 25 ºC (i.e. room temperature); and for the hot system two stages, with pre cure at room temperature for 10 hours, followed by a post cure at 80 ºC for 7 hours. Initially, the layers of E-glass mat (450 g/m^2), as well as the wires, are cut and weighted in a digital scale and their total mass, m_f and m_w, respectively, are registered. When the specimens are extracted from the molds their total weight, m_T, is measured. With these values, it is possible to calculate the mass of matrix, m_m, and the respectively mass fractions of matrix, fibers and wires. In addition, with the densities of the constituents it is possible to obtain the respective volume fractions, Vf, V_w and V_m.

The SMAHC beams, with 19 plies, were fabricated in the aluminum U shape female mold, which was previously covered with a layer of release wax. The typical cross section of the beams, with the geometric details incorporated, is presented in Fig. 3. The symmetric lamination starts with two layers of E-glass mat/epoxy, followed by one layer Ni-Ti /epoxy and thirteen (13) E-glass/epoxy plies. And, since the stacking sequence is symmetric about the middle surface (i.e. at t/2), the last layers of Ni-Ti/epoxy (1) and E-glass/epoxy (2) have the same materials and thickness as the initial ones (i.e. the number of plies, in sequence, is: 2+*1*+13+*1*+2, where the symmetric Ni-Ti layers are represented in bold and italic). Fig. 3 refers to a beam with 8 Ni-Ti wires, 4 above the middle surface and 4 below. The nominal length of all the six beams manufactured in this work was C = 300 mm and the width b = 31.3 mm.
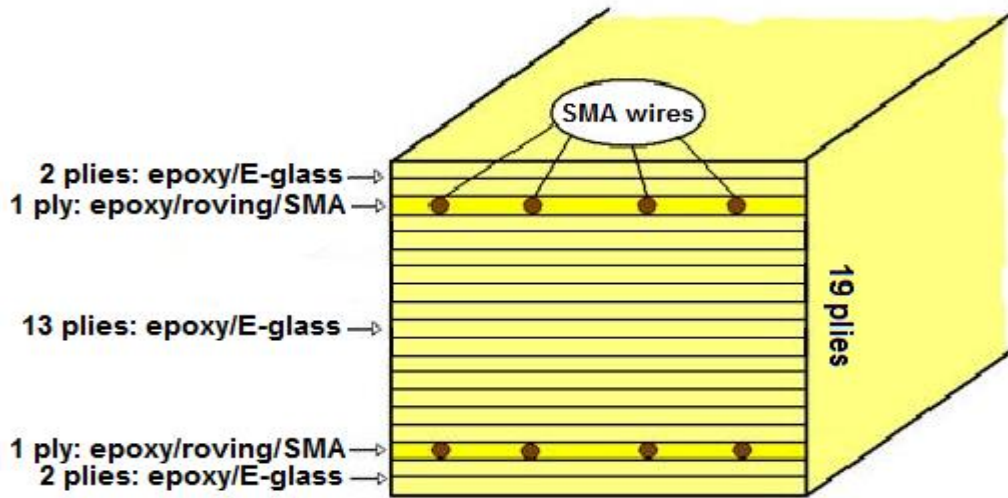
Figure 3. Cross-section views of the SMAHC beam with 19 plies

2.2   Mathematical modelling

Given a transverse vibration of an undamped Euler-Bernoulli beam it follows that the equation for natural frequency is given by Eq. (1) (Rao, 2008):

$$\omega_n = \frac{(\beta_n l)^2}{4\pi} \frac{t}{L^2} \sqrt{\frac{E_F 10}{3\rho_{beam}} 10^7}$$

(1)

In Eq. (1), the term ω_n is the nth transverse natural frequency of the beam. The $B_n l$ component is a factor that depends on the boundary condition and the vibration mode. L and t are respectively the length and the thickness of the beam, both in mm. E_F is the effective elastic modulus of the beam in GPa. ρ_{viga} is the density of the beam in kg/m^3. $\beta_n l$ values for the first 3 harmonics for free-free condition are given in Table 1 (Rao, 2008).

Table 1 – $\beta_n l$ values for free-free condition

$\beta_1 l$	$\beta_2 l$	$\beta_3 l$
4.730041	7.853205	10.995608

The effective elastic modulus (E_F) presented in Eq. (1) is the effective modulus of elasticity in bending of the symmetrical laminate beam. That is, an isotropic beam with elastic modulus of E_F, with the same geometry and subjected to the same load will present the same elastic deflections that the analyzed beam. The E_F module is shown in Eq. (2) (Levy Neto & Pardini, 2006).

$$E_F = \frac{8}{t^3} \sum_{j=1}^{\frac{N}{2}} (E_x)_j (z_j^3 - z_{j-1}^3)$$

(2)

In Eq. (2), $(E_x)_j$ is the modulus of elasticity of a generic ply j, z_j is the top coordinate of a ply from the middle plane of the beam, z_{j-1} is the bottom coordinate of a ply from the middle plane of the beam and N is the total number of beam plies.

According to Eq. (2) to obtain E_F it is necessary to calculate the elastic modulus of each ply of the SMAHC beam (see Fig. 3). The modulus of elasticity of the plies reinforced with chopped E-glass mat and epoxy ($E_{ChoppedEpoxyPly}$) depends on the volume fraction of fibers in the ply ($V_{FibersChoppedEpoxyPly}$) and is presented by Eq. (3) (Mendonça, 2005).

$$E_{ChoppedEpoxyPly} = 3.44 + 28.2\, V_{FibersChoppedEpoxyPly} + 21.6\, V_{FibersChoppedEpoxyPly}^{4} \tag{3}$$

The rule of mixtures is applied to calculate the modulus of elasticity in the direction of the wires (direction 1) of the plies reinforced with SMA wires, roving and epoxy. As the wires can vary its modulus of elasticity according to its phase (austenitic and martensitic), the modulus of elasticity in the direction of the wires containing them when they are in the austenitic phase ($E_{WiresPly\ Austenitic-1}$) and martensitic phase ($E_{WiresPly\ Martensític-1}$) are given respectively by Eqs. (4) and (5).

$$E_{WiresPly\,Austenitic-1} = E_{WiresAustenitic}V_{WiresPly} + E_{Roving}V_{FibersWiresPly} + E_{Matrix}V_{MatrixWiresPly} \tag{4}$$

$$E_{WiresPly\,Martensitic-1} = E_{WiresMartensitic}V_{WiresPly} + E_{Roving}V_{FibersWiresPly} + E_{Matrix}V_{MatrixWiresPly} \tag{5}$$

In Eqs. (4) and (5) $E_{WiresAustenit}$ and $E_{WiresMartensitic}$ are respectively the modulus of elasticity of the wires in the austenitic and martensitic phases. $V_{WiresPly}$ is the volume fraction of wires in the ply. E_{Roving} is the modulus of elasticity of the roving cables. $V_{FibersWiresPly}$ is the volume fraction of the fibers in the ply. E_{Matrix} is the modulus of elasticity of the matrix. $V_{MatrixWiresPly}$ is the volume fraction of matrix in the ply.

For further details on the formulation adopted in mathematical formulation, see "Ferreira, 2012".

2.2.1 Numerical simulations

The numerical analysis to characterize the dynamical behavior of the confectioned SMAHC beams was carried out using the software Abaqus®, which is a commercial finite element package. The simulations serve as support for the comparison, from a dynamic point of view, between the different manufacturing processes used and have the purpose to verify the effectiveness of the proposed analytical formulation, as well.

The beams were modeled in two different ways: **i)** as isotropic beams, based on the results obtained from the previously presented analytical formulation; and **ii)** using all its plies with specific propertied for each one.

When modeled as isotropic beams, only finite elements C3D8 type were used do discretize them in Abaqus®. The element used is a linear hexahedral (8 nodes) with full integration. Models contained approximately 1,000,000 nodes and 950,000 elements. Figure 4 presents a side view of one of the beams modeled as an isotropic beam.

The discretization of the beams with all plies was performed using mainly the finite element type C3D8 and secondarily the type C3D6. The second type of element is a linear triangular prism (6 nodes) with 2 points of integration. Approximately, these meshes contained 1,400,000 nodes and 1,100,000 elements. Figure 5 shows a side view of one of these meshed beams.
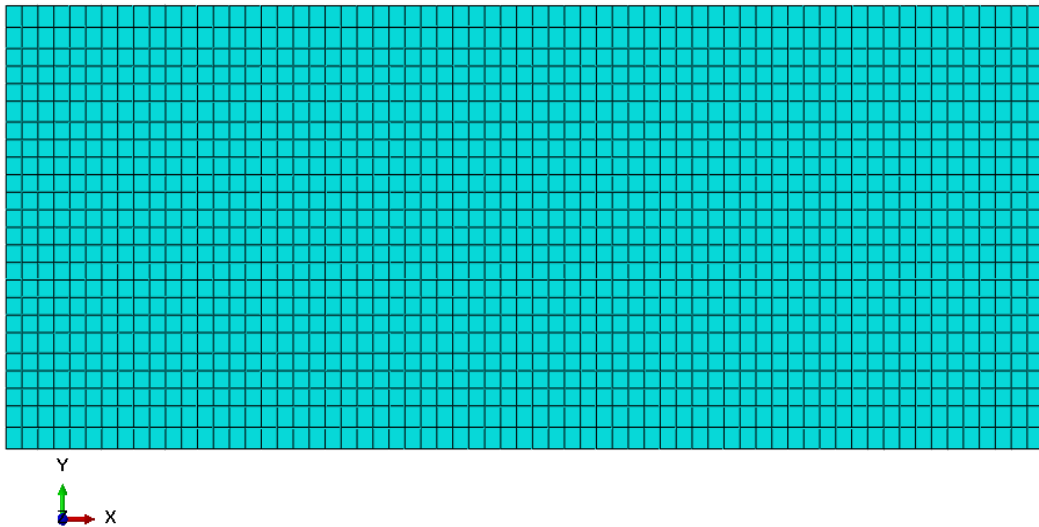
Figure 4. Cross-sectional view of one of the beams discretized as isotropic
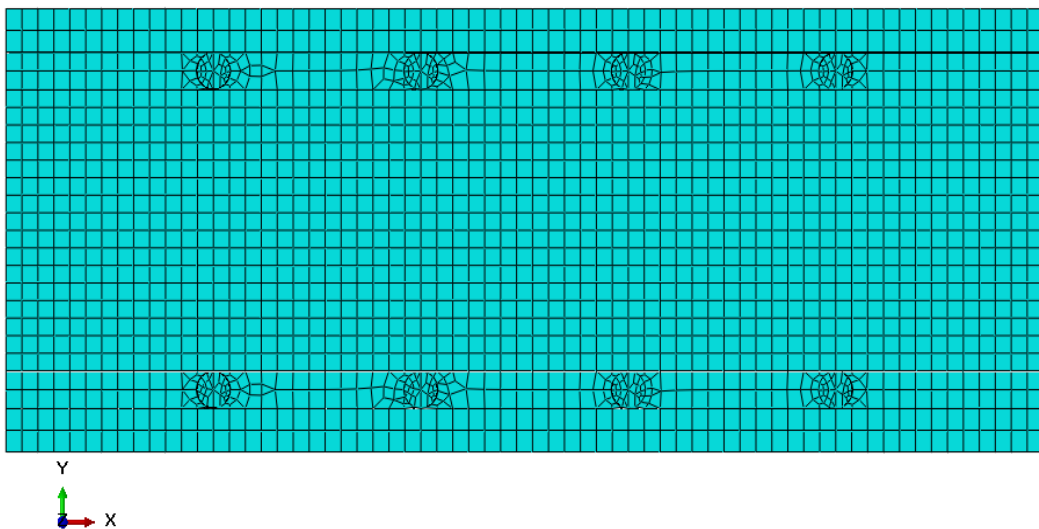

Figure 5. Cross-sectional view of one of the beams discretized with all plies

To model the SMAHCs beams it was necessary to determine the density and the modulus of elasticity, in the direction of the wires of each ply (see Fig. 3). To join the components of the molded beams the constraint conditions of type tie were used.

Similarly, the analytical formulation, has the purpose to obtain the natural frequencies of the first three transverse vibration modes of each of the beam from numerical simulations. Figures 6a, 6b and 6c show the displacements observed during transverse vibration modes analyzed from one of the examined beams.
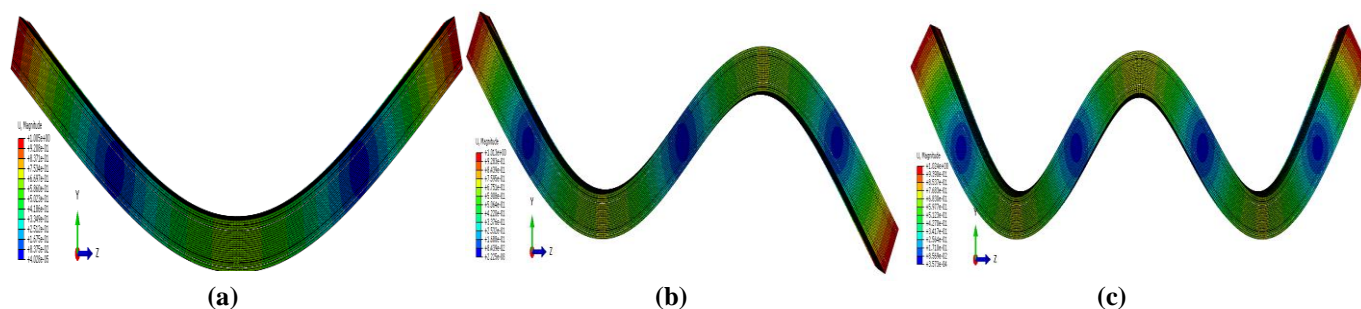
Figure 6. Displacements for the 1st (a), 2nd (b) e 3rd (c) transverse vibration modes of one of the simulated beams

3   RESULTS

Table 2 presents the identification of the manufactured beams according to the amount of wires (4, 6 or 8), the type of cure cycle (hot or cold) and vacuum type (absent, laboratory, or Hot Bonder device).

**Table 2. Identification of the manufactured beams**

Beam	Number of Wires	Cure Cycle	Vacuum
1	8	Cold	Absent
2	8	Hot	Absent
3	8	Cold	Absent
4	8	Hot	Laboratory
5	6	Hot	Laboratory
6	8	Hot	Hot Bonder device
7	4	Hot	Hot Bonder device

Table 3 shows the length, average thickness, width, weight, the amount of chopped E-glass and the amount of roving of each beam. The variations found in the thicknesses and weights of the constituents reflect the differences between the methods of manufacturing employed.

CILAMCE 2016

Proceedings of the XXXVII Iberian Latin-American Congress on Computational Methods in Engineering
Suzana Moreira Ávila (Editor), ABMEC, Brasília, DF, Brazil, November 6-9, 2016

Table 3. Average data of the beams

Beam	Length [mm]	Average Thickness [mm]	Width [mm]	Weight [g]	Chopped E-glass [g]	Roving [g]
1	299.16	12.29	31.55	180.0	67.5	0.0
2	298.90	12.66	31.47	182.0	64.5	0.0
3	300.18	14.37	31.39	208.0	72.5	5.5
4	299.31	11.41	31.43	174.0	71.5	13.5
5	300.17	11.49	31.50	173.0	71.0	10.0
6	299.84	12.40	31.47	177.5	72.0	10.0
7	300.16	8.93	31.48	131.0	71.0	10.0

Figures 7, 8 and 9, respectively, show the results obtained from the analytical formulation, from numerical simulations with effective modulus of elasticity (E_F) and numerical simulations with all plies. All results were generated using free-free boundary condition.
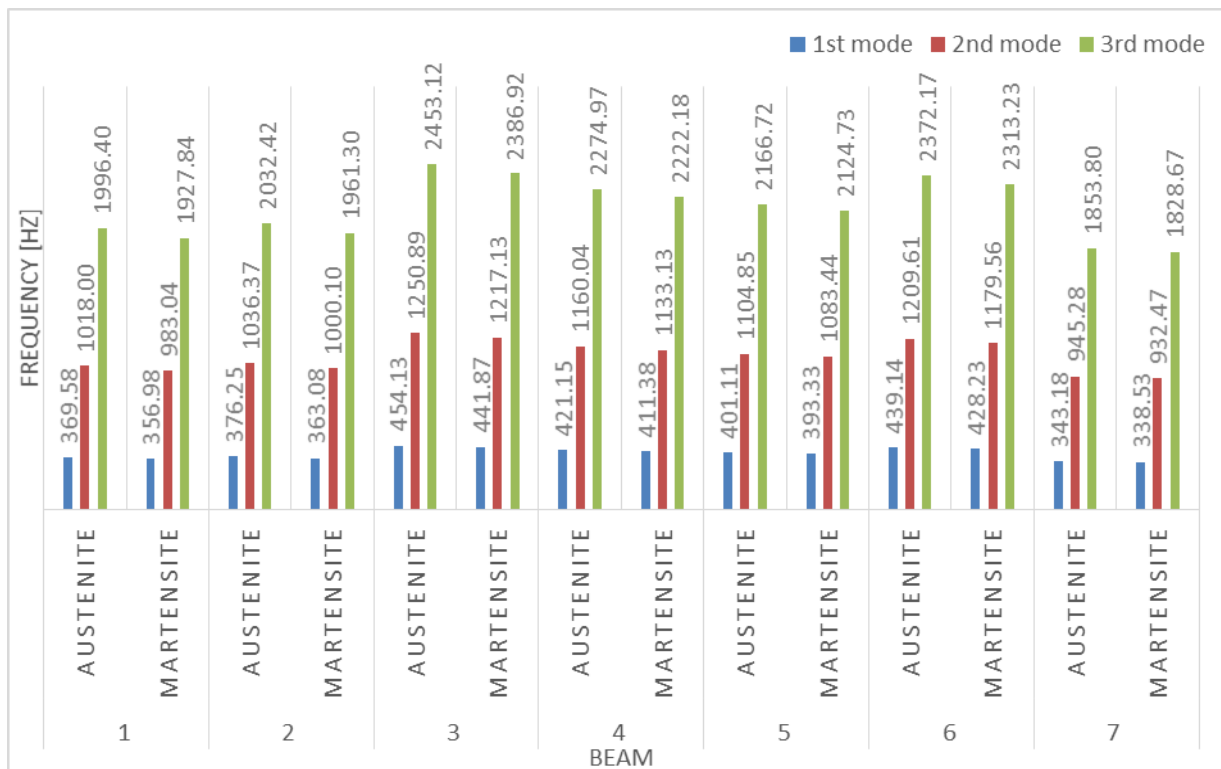
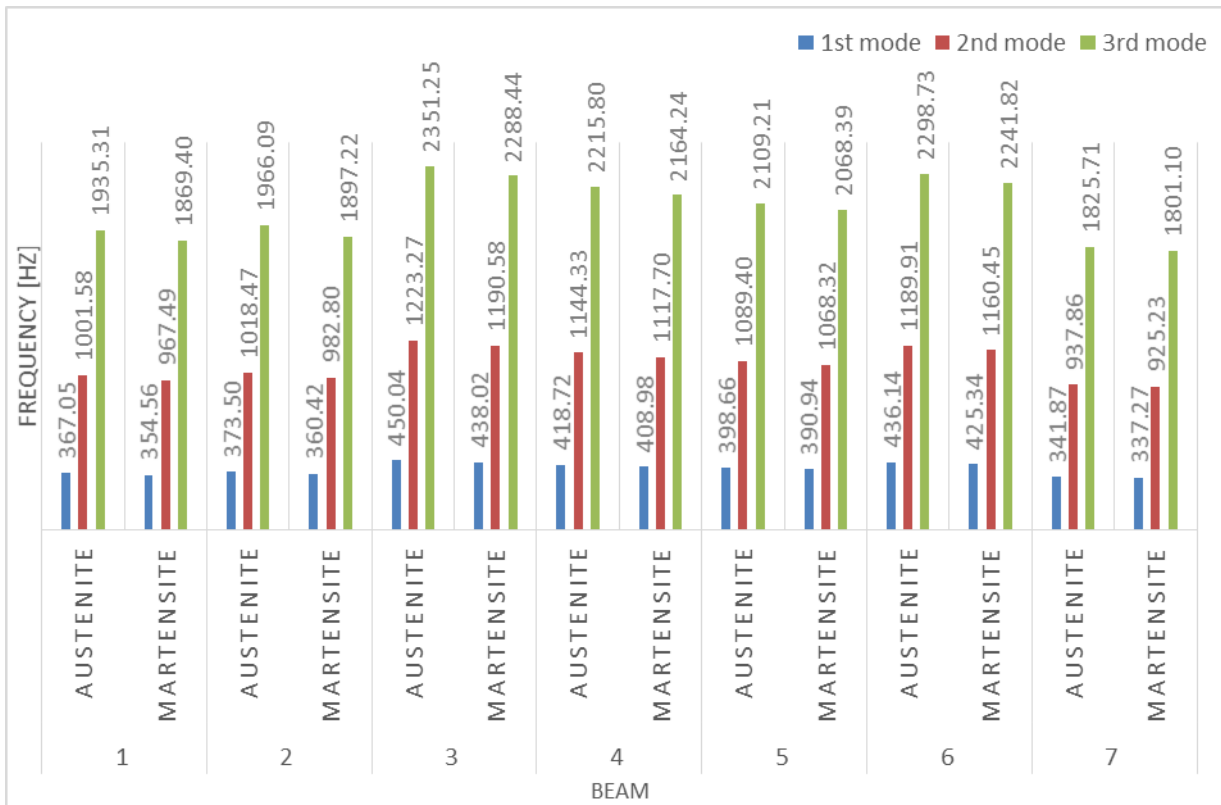**Figure 7. Natural frequencies obtained from the analytical formulation**

Figure 8. Natural frequencies obtained from the numerical simulations with E_F
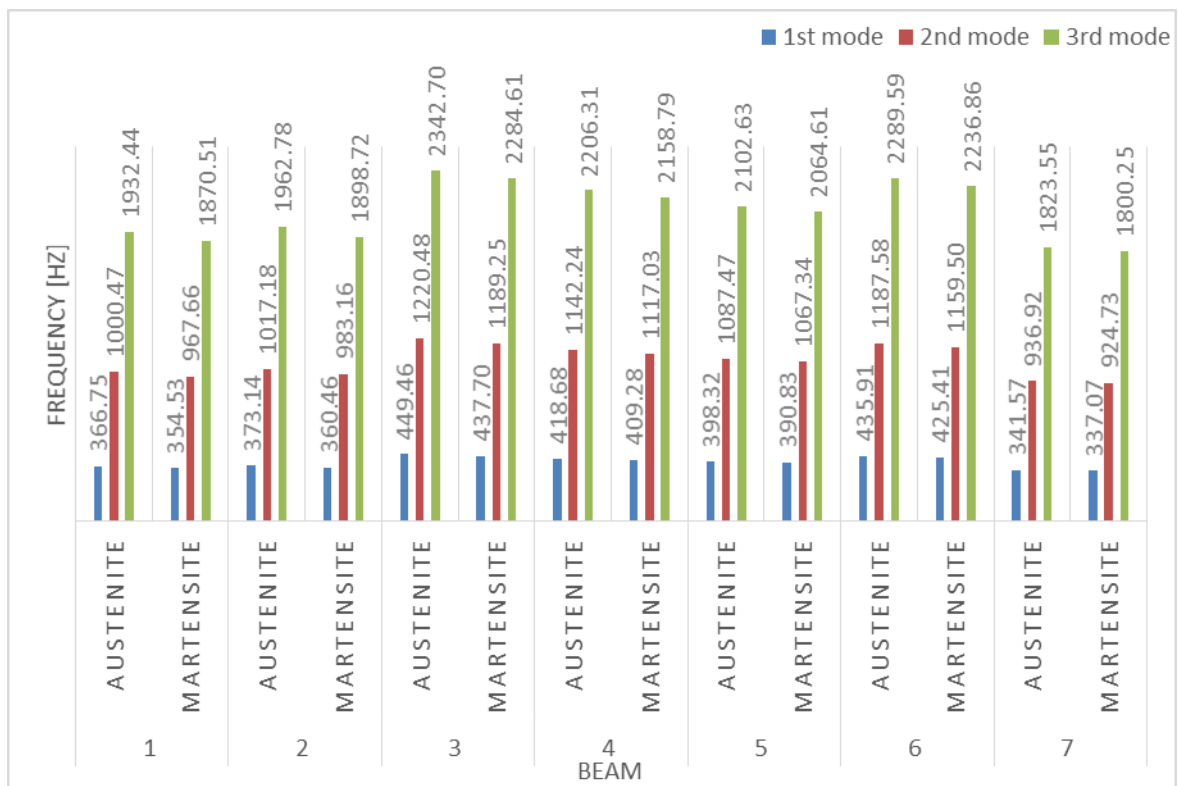

Figure 9. Natural frequencies obtained from the numerical simulations with all plies

Percentage differences between results obtained from numerical simulations, with E_F and those from the analytical formulation are presented in Fig. 10. Figure 11 shows percentage differences between numerical results with all plies and analytical results. Finally, Fig. 12 presents percentage differences between results from numerical simulation with all plies and those from numerical simulations with E_F.

Figure 10. Percentage differences between results from numerical simulation with E_F and those from analytical formulation
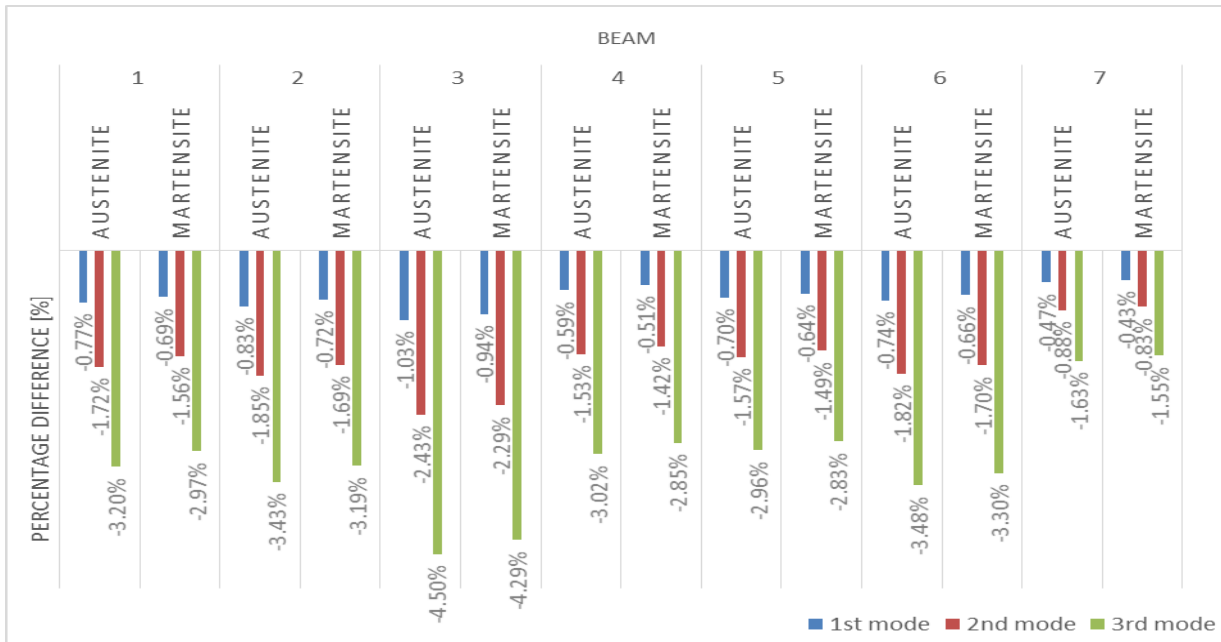

Figure 11. Percentage differences between results from numerical simulation with all plies and those from analytical formulation
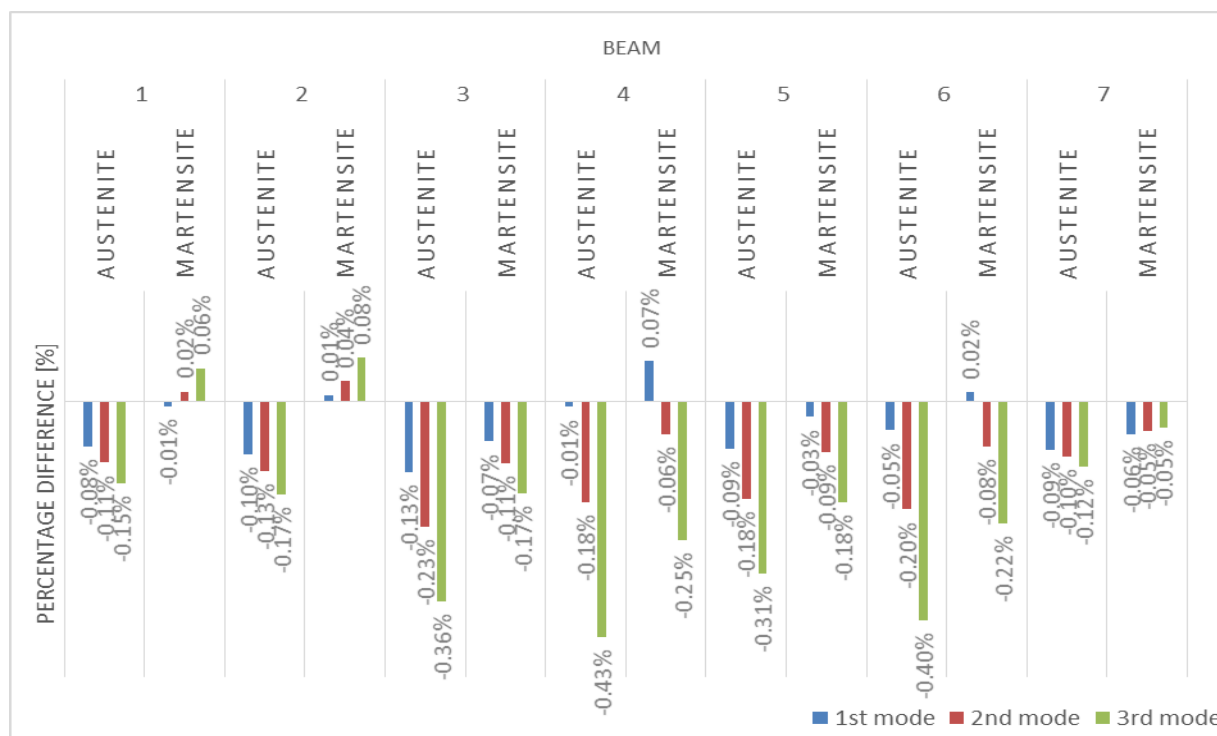
Figure 12. Percentage differences between results from numerical simulation with all plies and those from numerical simulation with E$_F$

4   ANALYSIS OF RESULTS AND CONCLUSIONS

4.1   Analysis of results

From Fig. 7, based on analytical, it is observed that beam 7 had lowest natural frequencies, taking into account the first three vibration modes (343.18 Hz, 945.28 Hz and 1853.80 Hz for austenitic phase; 338.53 Hz, 932.47 Hz and 1828.67 Hz for martensitic phase). On the other side, beam 3 showed highest natural frequencies (454.13 Hz, 1250.89 Hz and 2453.12 Hz for austenitic phase; 441.87 Hz, 1217.13 Hz and 2386.92 Hz for martensitic phase).

Numerical simulations adopting the equivalent isotropic flexural modulus, E$_F$ (see Fig. 8), showed that lowest natural frequencies were found on beam 7 (341.87 Hz, 937.86 Hz and 1825.71 Hz for austenitic phase; 337.27 Hz, 925.23 Hz and 1801.10 Hz for martensitic phase). And highest natural frequencies for beam 3 (450.04 Hz, 1223.27 Hz and 2351.25 Hz for austenitic phase; 438.02 Hz, 1190.58 Hz and 2288.44 Hz for martensitic phase).

Results of numerical simulations, with all discrete layers considered in the analysis (see Fig. 9), presented similar behavior to that described above, i.e., beam 7 had lowest natural frequencies (341.57 Hz, and 936.92 Hz and 1823.55 Hz for austenitic phase; 337.07 Hz, 924.73 Hz 1800.25 Hz for martensitic phase) and beam 3 had highest natural frequencies (449.46 Hz, 1220.48 Hz and 2342.70 Hz for austenitic phase; 437.70 Hz, 1189.25 Hz 2284.61 Hz for martensitic phase).

CILAMCE 2016

Proceedings of the XXXVII Iberian Latin-American Congress on Computational Methods in Engineering
Suzana Moreira Ávila (Editor), ABMEC, Brasília, DF, Brazil, November 6-9, 2016

Analyzing Fig. 10, it is observed that, in module, lowest percentage differences between numerical simulations with E_F and those obtained from analytical formulation, were found on beam 7 (-0.38%, -0.78% and -1.52% for austenitic phase; -0.38%, -0.78% and -1.51% for martensitic phase) and highest ones were found on beam 3 (-0.90%, -2.21% and -4.15% for austenitic phase; -0.87%, -2.18% and -4.13% for martensitic phase).

Observing Fig. 11, it is noticed that, in module, beam 7 also presented lowest percentage differences (-0.47%, -0.88% and -1.63% for austenitic phase; -0.43%, -0.83% and -1.55% for martensitic phase) and beam 3 showed highest ones as well (-1.03%, -2.43% and -4.50% for austenitic phase; -0.94%, -2.29% and -4.29% for martensitic phase).

Comparing numerical simulations employed it can be seen that, in module, the lowest percentage difference was 0.01% (1st modes of beams 1, 2 and 4 – all of them in the martensitic phase) and the highest was 0.43% (3rd mode of beam 4 in the austenitic phase).

4.2   Conclusions

Analytical results obtained from the formulation proposed in this work and the numerical simulations showed a similar qualitative behavior, that is, phase transformation of the Ni-Ti wires alters natural frequencies of all the beams and the ordination of beams in terms of the values of natural frequencies remained the same for all methods.

In module, highest percentage differences of numerical simulations were found in the 3rd mode of beam 3 in the austenitic phase (-4.15% for simulation with E_F and -4.50% for simulation with all plies). These percentage differences are within a reasonable limit in terms of engineering (something below 5%). Furthermore, it is important to mention that the highest percent differences between numerical methods and analytical solution were found to the highest values of natural frequencies, that is, for higher vibration modes and for the beams that had intricately high natural frequencies.

Given the excellent correlation between the numerical methods (in module, the highest percentage difference was 0.43% to the 3rd mode of beam 4 in the austenitic phase) it can be concluded that the modeling with effective modulus of elasticity, E_F, is very robust and therefore recommended. Additionally, computational cost is significantly reduced when the model with isotropic beam is used (approximately 95% faster).

All vibration modes and natural frequencies discussed in this study took into account free-free boundary condition. However, manufactured beams are able, in principle, to act satisfactorily when subjected to other boundary conditions (fixed-free and fixed-fixed, for example).

Usage of vacuum decreased the amount of epoxy presented in the laminate, as a result two important phenomena could be observed. The first was the distance reduction from the neutral line to the ply that contains wires. As this distance (z) is cubed (z^3 in the formula for obtaining the effective modulus of elasticity, see Eq. (2)), the influence of the change of the modulus of elasticity of the wires between the austenitic phase (hot) and martensitic phase (cold) was reduced. The second important factor noted is that the volume fraction of glass fiber (E = 70 GPa) was increased, and this also makes the effect of phase change of wires less pronounced. The last factor is mainly because the modulus of elasticity found in the plies composed only by chopped E-glass and epoxy becomes quite high and ended masking the effect of phase transformation of the wires. The absence of roving (E=70 GPa) and non-use of vacuum highlighted more strongly the phase transformation of the SMA wires, which causes the increase in the modulus of elasticity of Ni-Ti wires.

The type o cure cycle (hot or cold) did not affect the results. Therefore, it has to be defined taking into account the application of the material. Beams with hot cure should be used at higher temperature conditions and also under conditions where the wires of Ni-Ti must be heated several times. Usage of heat cure also aims to reduce creep effects in the material. The process using hot cure is more expensive, but the cure of epoxy resin is faster at a higher temperature.

ACKNOWLEDGEMENTS

REFERENCES

Daniel, I. M., & Ishai, O., 2006. *Engineering Mechanics of Composite Materials*, 2nd ed., University Press, Oxford, United Kingdom.

Faluhelyi, P., 2013. *Fabricação e Comportamento Termomecânico de Compósitos Estruturais Adaptativos de Liga Ni-Ti*, PhD Thesis, Departament of Mechanical Engineering , Faculty of Technology, University of Brasília, Brasília, Distrito Federal, Brazil.

Ferreira, G. V., 2012. *Fabricação e Análise Modal de Vigas Híbridas Compósitas*, Graduation Project, Departament of Mechanical Engineering , Faculty of Technology, University of Brasília, Brasília, Distrito Federal, Brazil.

Ghandi, M. V., & Thompson, B. S., 1992, *Smart Materials and Structures*, Chapman e Hall, London, United Kingdom.

Janocha, H., 1999, *Adaptronics and smart structures – Basics, materials, design and applications,* 1999, Springer – Verlag, Berlin Heidelberg, New York, United States.

Levy-Neto, F. & Pardini, L. C., 2006. *Compósitos estruturais: Ciência e Tecnologia*, 1ª Ed, Ed. Edgard Blücher, São Paulo, Brazil.

Mendonça, P. T. R., 2005. *Materiais Compostos & Estruturas-Sanduíche: Projeto e Análise*, Ed. Manole, Barueri, São Paulo, Brazil.

Otsuka, K. & Wayman, C. M, 1998, *Mechanism of Shape Memory Effect and Superelasticity*, In.: OTSUKA, K.; WAYMAN, C. M. (Eds) Shape Memory Materials, Cambridge University Press, Cambridge, United Kingdom.

Rao, S. S., 2008. *Vibrações Mecânicas*, 4ª Ed, Ed. Pearson Prentice Hall, São Paulo, Brazil.

Rogers, C. A., & Robertshaw, H. H., 1989, *Shape memory reinforced composites*, Engineering Science Preprints 25, Soc. Of Engineering Sciences.

Silva, J. P. C., 2009. *Fabricação e Análise de Vigas Adaptativas com Filamentos de Liga de Níquel-Titânio*, Graduation Project, Departament of Mechanical Engineering , Faculty of Technology, University of Brasília, Brasília, Distrito Federal, Brazil.

Srinivasan A. V., & McFarland, M. D., 2001. *Smart Structures Analysis and Design*, Cambridge University Press, Cambridge, United Kingdom.

Turner, T.L., 2001. *Thermomechanical Response of Shape Memory Alloy Hybrid Composites*. NASA/TM-2001-210656, Langley Research Center, Hampton, Virginia, United States.

www.matweb.com, accessed on March 2016; E-glass fiber properties.